

# FISSION OF COLLAPSING CAVITATION BUBBLES

Christopher E. Brennen

California Institute of Technology, Pasadena, CA 91125

## Abstract

High-speed observations (for example, Lauterborn and Bolle 1975, Tomita and Shima 1990, Frost and Sturtevant 1986) clearly show that though a collapsing cavitation bubble approaches its minimum size as a coherent single volume, it usually reappears in the first rebounding frame as a cloud of much smaller bubbles or as a highly distorted single volume (see, for example, figure 2). This paper explores two mechanisms that may be responsible for that bubble fission process, one invoking a Rayleigh-Taylor stability analysis and the other utilizing the so-called microjet mechanism. Both approaches are shown to lead to qualitatively similar values for the number of fission fragments and the paper investigates the flow parameters that effect that number. Finally, we explore the effective damping of the Rayleigh-Plesset single bubble calculation which that fission process implies and show that it is consistent with the number of collapses and rebounds which are observed to occur in experiments.

## 1 Introduction

Rayleigh-Plesset calculations for cavitation bubbles are now commonly embedded in efforts to computationally simulate cavitating flows. The implicit assumption is that the bubble remains sufficiently spherical for this equation to adequately represent its dynamic volumetric behavior. When the latter is compared with experimental observations, there are many respects in which this approximation proves acceptable, particularly during the growth of the bubble to its maximum size and the initial part of the collapse phase. However, most high-speed observations of the collapse show that the bubble fissions during passage through its minimum volume and, thereafter, the Rayleigh-Plesset analysis fails to accurately predict the dynamic behavior. In part this is because the Rayleigh-Plesset equation fails to represent the energy dissipation associated with the fission process. As a consequence, the number and strength of the rebounds observed in the experiments are much smaller than predicted by the calculations.

## 2 Collapse Relations

However, before investigating the fission process, it is necessary to establish the essential features of the growth and collapse of a cavitating bubble as it passes through a low pressure region in the flow. For this purpose we use the approximate relations that are derived from the classical Rayleigh-Plesset model and presented in Brennen (2001). It is assumed that thermal effects may be neglected, that the mass of non-condensable gas in the bubble remains constant and that the behavior of that gas can be represented by a polytropic constant,  $k$ . Then the Rayleigh-Plesset equation (see, for example, Brennen 1995) connecting the time-dependent bubble radius,  $R(t)$ , to the pressure in the liquid,  $p_\infty(t)$ , is

$$\frac{p_V - p_\infty(t)}{\rho} + \frac{p_{G_o}}{\rho} \left\{ \frac{R_o}{R} \right\}^{3k} = R\ddot{R} + \frac{3}{2}(\dot{R})^2 + \frac{4\mu_e\dot{R}}{\rho R} + \frac{2S}{\rho R} \quad (1)$$

where  $p_V$  is the vapor pressure at the prevailing temperature,  $p_{G_o}$  is the partial pressure of non-condensable gas in the initial cavitation nucleus,  $\rho$  and  $S$  are the liquid density and the surface tension and the overdot denotes  $d/dt$ . For the moment,  $\mu_e$ , can be considered to be the liquid viscosity.

For the purposes of the present investigation we consider a single cavitation nucleus of radius  $R_o$  initially at equilibrium at the initial liquid pressure  $p_\infty^i$ . It follows that the initial partial pressure of gas is given by  $p_{Go} = p_\infty^i - p_V + \frac{2S}{R_o}$ . This nucleus is then subjected to an episode in which the liquid pressure is decreased below the vapor pressure,  $p_V$ , causing explosive cavitation growth of the bubble to a radius much larger than  $R_o$ . The ambient pressure eventually increases again, causing the bubble to collapse violently.

In Brennen (2001) we develop approximate analytical expressions for some of the main features of the bubble dynamics. The focus is on that very brief instant at the heart of the collapse when the bubble radius becomes very much smaller than  $R_o$ . We first define a typical duration for the reduced pressure interval,  $t_R$ , and a typical tension,  $p_V - p_\infty^m$ , under which growth occurs so that

$$R_{max} \approx \left\{ \frac{2(p_V - p_\infty^m)t_R^2}{3\rho} \right\}^{\frac{1}{2}} \quad (2)$$

During the initial part of the collapse the acceleration,  $\ddot{R}$  is negative. However later in the collapse this acceleration changes sign as the noncondensable gas inside the bubble begins to be compressed. Defining the origin of our time frame,  $t = 0$ , to be the moment of minimum bubble size, we shall refer to the moment at which  $\ddot{R} = 0$  as the beginning of the rebound and denote it by  $t = -t_*$ . It is readily demonstrated that if the ambient pressure at collapse is  $p_\infty^c$  then the minimum bubble radius,  $R_{min}$ , at  $t = 0$  is given by

$$\frac{R_{min}}{R_o} = \left\{ \frac{2R_o^3 p_{Go}}{3\rho(k-1)K} \right\}^{\frac{1}{3(k-1)}} \quad \text{where} \quad K \approx 2(p_\infty^c - p_V)R_{max}^3/3\rho \quad (3)$$

Moreover, the radius,  $R_*$ , and radial velocity,  $\dot{R}_*$ , at the beginning of the rebound are given by

$$R_* = (k)^{\frac{1}{3(k-1)}} R_{min} \quad \text{and} \quad \dot{R}_* = \left\{ \frac{(k-1)K}{kR_*^3} \right\}^{\frac{1}{2}} \quad (4)$$

To parameterize these results, we define a Thoma cavitation number,  $\sigma$ , which describes how close the inlet pressure is to the vapor pressure and a non-dimensional pressure distribution characteristic,  $\alpha$ , as follows:

$$\sigma = (p_\infty^i - p_V)/(p_\infty^i - p_\infty^m) \quad ; \quad \alpha = (p_\infty^c - p_\infty^m)/(p_\infty^i - p_\infty^m) \quad (5)$$

The parameter  $\alpha$  will be a characteristic of the geometry of the flow regardless of the vapor pressure and will often taken a value of the order of unity. Then the surface tension,  $S$ , and the residence time,  $t_R$ , are conveniently represented by the parameters:

$$R_o^* = \frac{R_o(p_\infty^i - p_\infty^m)}{S} \quad ; \quad C_P = \frac{t_R}{R_o} \left\{ \frac{2(p_\infty^i - p_\infty^m)}{3\rho} \right\}^{\frac{1}{2}} \quad (6)$$

Note that in the expressions 5 and 6 the pressure difference ( $p_\infty^i - p_\infty^m$ ) has been uniformly used as one of the non-dimensionalizing factors. In addition, we introduce a combination parameter which will appear in several places in the results ahead, namely

$$C_Q = C_P(k-1)^{\frac{1}{3}}(\alpha-1+\sigma)^{\frac{1}{3}}(1-\sigma)^{\frac{1}{2}} \quad (7)$$

Then it follows that

$$\frac{R_{max}}{R_o} = \frac{C_P}{(1-\sigma)^{\frac{1}{2}}} \quad ; \quad \frac{R_{min}}{R_o} = (\sigma + 2/R_o^*)^{\frac{1}{3(k-1)}} C_Q^{-\frac{1}{(k-1)}} \quad ; \quad K = \frac{2R_o^3 C_Q^3 (p_\infty^i - p_\infty^m)}{3\rho(k-1)} \quad (8)$$

### 3 Stability to Spherical Harmonic Distortion

The stability of cavitating bubbles to nonspherical disturbances has been investigated analytically by Birkhoff (1954), Plesset and Mitchell (1956), Brennen (1995) among others. These analyses examined the spherical

equivalent of the Rayleigh-Taylor instability. If the inertia of the gas in the bubble is assumed to be negligible, then the amplitude,  $a(t)$ , of a spherical harmonic distortion of order  $n$  ( $n > 1$ ) is governed by the equation:

$$\frac{d^2 a}{dt^2} + \frac{3}{R} \frac{dR}{dt} \frac{da}{dt} - \left\{ \frac{(n-1)}{R} \frac{d^2 R}{dt^2} - (n-1)(n+1)(n+2) \frac{S}{\rho R^3} \right\} a = 0 \quad (9)$$

Note that the coefficients require knowledge of the global dynamic behavior,  $R(t)$ . The fact that they are not constant in time causes departure from the equivalent Rayleigh-Taylor instability for a plane boundary. However, the coefficient of  $a$  within the parentheses,  $\{\}$ , of equation 9 is not greatly dissimilar from the case of the plane boundary in the sense that instability is promoted when  $\ddot{R} > 0$  and surface tension has a stabilizing effect. Plesset and Mitchell (1956) examined the particular case of a vapor/gas bubble initially in equilibrium that is subjected to a step function change in the pressure at infinity. Later calculations by Brennen (1995), incorporated the effect of the noncondensable gas in the bubble. The effect of the gas is essential for present purposes since its compression causes the rebound and the instability that is addressed here.

It is clear from equation 9 that the most unstable circumstances occur when  $\dot{R} < 0$  and  $\ddot{R} \geq 0$ . These conditions are met following the beginning of the rebound (as defined earlier) and result in very rapid growth in non-spherical distortion. This leads to the very rapid disintegration of the bubble and its metamorphosis into the cloud of smaller bubbles which is seen in experiments to emerge from the collapse of the bubble. The growth rate of the distortions is controlled by the magnitude of the term in the parentheses,  $\{\}$ , in equation 9. The larger the value of this term the greater the growth rate. Note that  $n$  occurs only in this term and that the functional dependence on  $n$  has the form  $(n-1) \{\Gamma - (n+1)(n+2)\}$  where  $\Gamma = \rho R^2 \dot{R}/S$ . It follows that as long as  $\Gamma$  is positive, there will be a particular value of  $n$  (denoted by  $n_m$ ) for which the term has a positive maximum. We would expect this mode of distortion to dominate and therefore to play a role in determining the number of fission bubbles. Parenthetically we note that Shepherd (1980) follows a qualitatively similar argument in an effort to predict the wavelengths of surface distortion seen on the bubbles in the same experiments from which figure 2 was taken.

One complicating factor is that  $\Gamma$  will vary with time within the unstable interval increasing from zero at  $t = -t_*$  to a maximum  $\Gamma_m$  when  $R = R_{min}$ . Clearly, however,  $\Gamma_m$  is a representative value and can be written in terms of the parameters defined in section 2:

$$\Gamma_m = \frac{R_o^* C_Q^{\frac{3k-1}{(k-1)}}}{(\sigma + 2/R_o^*)^{\frac{2}{3(k-1)}}} \quad (10)$$

Then, taking  $\Gamma_m$  as the characteristic value of  $\Gamma$ , the most unstable mode is

$$n_m = \left\{ (7 + 3\Gamma_m)^{\frac{1}{2}} - 2 \right\} / 3 \quad \text{and} \quad n_m \approx \left\{ \frac{\Gamma_m}{3} \right\}^{\frac{1}{2}} = \frac{(R_o^*)^{\frac{1}{2}} C_Q^{\frac{3k-1}{2(k-1)}}}{3^{\frac{1}{2}} (\sigma + 2/R_o^*)^{\frac{1}{3(k-1)}}} \quad (11)$$

provided  $n_m \gg 1$ . We note that  $n_m \approx (\Gamma_m/3)^{\frac{1}{2}}$  is functionally similar to the most unstable surface distortion wavelength prediction included in the analysis of Shepherd and Sturtevant (1982).

Given the most unstable Rayleigh-Taylor mode, the next question is to estimate the number of fission fragments which that mode might lead to. Assuming that the fission fragment size is directly related to the wavelength of the distortion on the surface of the whole bubble, a crude estimate would be that the fragment radius,  $R_F$ , would be given roughly by  $R_F = R/n_m$ . Then if the original volume is equally divided amongst these fragments it follows that the number of fission fragments is  $n_m^3$ . We delay discussion of this result until an alternative approach is examined.

## 4 Jet Breakup

The results at the end of the last section assumed a particular model of bubble fission. In another set of circumstances, it has been observed that a bubble collapsing close to a wall or free-surface forms a re-entrant jet which shatters the bubble into many fragments when the jet impacts the other side of the bubble surface.

In this section we seek to estimate the number of fission fragments that would result from this mode of bubble disintegration. To do so crudely we estimate that the size of the bubbles that survive such a violent process are those for which the surface tension forces holding the fission fragment together are roughly equal to the shear forces tearing it apart. The shear rates involved could be estimated as  $\gamma = \dot{R}/R$  at the beginning of the rebound and, from equations 4,  $\dot{R}$  can be estimated as  $\dot{R}_*$  where

$$\dot{R}_*^2 = \frac{\{R_o C_P / t_R\}^2 \{C_Q / k^{\frac{1}{3}}\}^{\frac{3k}{(k-1)}}}{\{\sigma + 2/R_o^*\}^{\frac{1}{(k-1)}}} \quad (12)$$

To estimate the fission fragment size,  $R_F$ , we could then equate the typical surface tension force,  $2\pi R_F S$ , to the typical shearing force,  $6\pi\mu\gamma R_F^2$  so that  $R_F = S/3\mu\gamma$ . It would then follow that the number of fission fragments would be  $n_j^3$  where

$$n_j = \frac{R_*}{R_F} = \frac{3\mu\dot{R}_*}{S} = \frac{6^{\frac{1}{2}} R_o^* \{C_Q / k^{\frac{1}{3}}\}^{\frac{3k}{2(k-1)}}}{C_\mu (\sigma + 2/R_o^*)^{\frac{1}{2(k-1)}}} \quad \text{where} \quad C_\mu = \frac{R_o \{\rho(p_\infty^i - p_\infty^m)\}^{\frac{1}{2}}}{\mu} \quad (13)$$

The shearing force,  $6\pi\mu\gamma R_F^2$ , used in deriving this result is a low Reynolds number formulation and requires that  $\rho\dot{R}_* R_* / \mu \ll 1$ . If, on the other hand,  $\rho\dot{R}_* R_* / \mu \gg 1$ , an appropriate estimate of the shearing force would be  $\pi\rho\gamma^2 R_F^4$ . Then it would follow that

$$n_j = \frac{R_*}{R_F} = \left\{ \frac{\rho\dot{R}_*^2 R_*}{2S} \right\}^{\frac{1}{3}} = \frac{(R_o^*)^{\frac{1}{3}} \{C_Q / k^{\frac{1}{3}}\}^{\frac{3k-1}{3(k-1)}}}{3^{\frac{1}{3}} (\sigma + 2/R_o^*)^{\frac{2}{9(k-1)}}} \quad (14)$$

It is fairly easy to demonstrate that if the viscous terms dominate the inertial terms and lead to expression 13 rather than expression 14 then the viscous terms in the Rayleigh-Plesset equation itself should have been included in the analysis of section 2. Since they were not so included, it follows that expression 13 is of dubious validity. Consequently, in the interest of brevity, we will not pursue the low bubble Reynolds number result any further.

In the next section we consider the consequences of the result 14.

## 5 Fission Fragments

In assessing the results of the last two sections, namely expressions 11, 13 and 14 for the number of fission fragments, we note that all three results have quite similar forms. This is because they all involve fission forces which are inertial in origin and a resistance to fission governed by surface tension. Moreover, since  $\sigma$  is often of order unity, the magnitude of  $n_m$  or  $n_j$  is primarily determined by the numerator and is therefore a function of  $R_o^*$  and  $C_Q$  (or, effectively,  $C_P$ ), though  $C_\mu$  also appears in the expression 13. Concentrating on those numerators involving  $R_o^*$  and  $C_Q$  we see that  $n_m$  and  $n_j$  sensibly decrease with increasing  $S$ . The variation with nuclei size is more complex and requires consideration of the factor  $(\sigma + 2/R_o^*)$  in the denominators. For very small nuclei sizes such that  $R_o^* \ll 2/\sigma$  the number of fission fragments increases with the nuclei size (provided  $k$  takes some reasonable number). However, for larger nuclei such that  $R_o^* \gg 2/\sigma$  the number of fission fragments *decreases* as the nuclei size increases. This slightly non-intuitive trend occurs because the maximum bubble size becomes essentially independent of the nuclei size; however, the larger nuclei contribute more non-condensable gas to the collapse and the collapse is therefore *less* violent leading to fewer fission fragments.

We will now illustrate the results for  $n_m$  and  $n_j$  with some numerical examples. In figure 1 values for  $n_m$  and  $n_j$  from the expressions 11 and 14 are plotted against the dimensionless nuclei size,  $R_o^*$ , for various values of the parameter,  $C_Q$ , and the cavitation index,  $\sigma$ . Note that for a typical surface tension,  $S$ , of  $0.07\text{kg/s}^2$  and a typical pressure difference,  $(p_\infty^i - p_\infty^m)$ , of  $10^5\text{kg/m s}^2$ , nuclei of radii,  $R_o$ , ranging from  $1\mu\text{m}$  to  $100\mu\text{m}$  would yield  $R_o^*$  values ranging from 1.4 to 140, roughly in the middle of the horizontal scale. Moreover, cavitation indices in the range used in the figures are commonly experienced. Perhaps the greatest

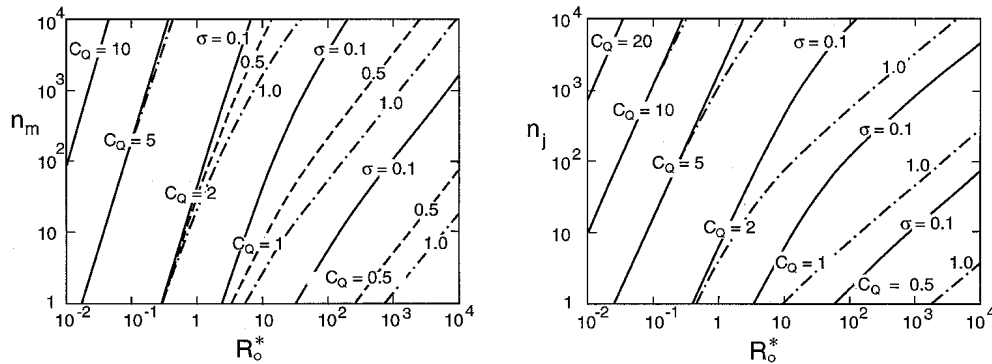


Figure 1: Left: values of  $n_m$  from the Rayleigh-Taylor instability analysis. Right: values of  $n_j$  from the re-entrant jet breakup analysis. Both plotted against  $R_o^*$  for  $k = 1.4$  and various values of the parameter,  $C_Q$ , and the cavitation number,  $\sigma$ .

uncertainty lies in estimating typical values of  $C_Q$  occurring in practice. The simplest way to estimate this is to use the first of equations 8. Common values of  $R_{max}/R_o$  range from 10 up to 100 and higher and this provides an estimate of  $C_P$ . The definition 7 suggests that  $C_Q$  will typically be about an order of magnitude smaller than  $C_P$  and this leads to an estimate of  $C_Q$  of order unity or greater. Figure 1 indicates that for  $C_Q = 1$  the smaller nuclei may lead to collapses without fission if the cavitation number is large enough. However, large nuclei at lower cavitation numbers will lead to breakup into large numbers of fission fragments.

## 6 Some Comparison with Observations

While many of the photographs of cavitation bubbles before and after the first collapse (for example, Lauterborn and Bolle 1975, Tomita and Shima 1990) show that the bubble has fissioned into many fragments, the photographs rarely have the kind of resolution that would allow a count of the number of those fragments. On the other hand, though they are not normal cavitation bubbles, the beautiful photographs of Frost and Sturtevant (1986) showing the breakup of ether vapor bubbles in glycerol are of sufficient resolution to allow comparison with the present analysis.

Frost and Sturtevant (1986) (see also, Shepherd and Sturtevant (1982), Shepherd (1980), Frost (1985)) allowed drops of ether in glycerol to explosively evaporate and then examined the surface appearance as the bubble oscillated. In addition they measured the pressures radiated as a result of these oscillations. Sample photographs just after either the first or second collapses are shown in figure 2. We counted the individual bubbles observable on the half-surface facing the camera. Doubling that number to account for the back side yielded values of 320, 400 and 410 respectively for the three cases. In the framework of section 3 this number should correspond to  $n_m^2$  and hence the photographs indicate  $n_m \approx 20$ .

To compare the theory of section 3, we note that the pressure radiated from an oscillating bubble has an amplitude,  $\tilde{p}$ , given roughly by

$$\tilde{p} = \frac{\rho}{4\pi\mathcal{R}} \frac{d^2V}{dt^2} \approx \frac{\rho R^2}{\mathcal{R}} \frac{d^2R}{dt^2} \quad (15)$$

where  $V$  and  $R$  are the volume and radius of the bubble and  $\mathcal{R}$  is the distance from the bubble center to the point of pressure measurement (see Brennen 1995). Substituting for  $R^2 d^2R/dt^2$  from the definition for  $\Gamma_m$  and using the approximation in equation 11 yields

$$n_m = \{\Gamma_m/3\}^{\frac{1}{2}} \approx \{\mathcal{R}|\tilde{p}|/3S\}^{\frac{1}{2}} \quad (16)$$

where  $|\tilde{p}|$  is the amplitude of the radiated pressure. From the pressure traces given by Frost(1985), we estimate the values of  $|\tilde{p}|$  for the three photographs in figure 2 to be  $6 \times 10^4 kg/ms^2$ . With this,  $\mathcal{R} = 6mm$  and  $S = 0.07N/m$ , equation 16 yields  $n_m = 41$ .

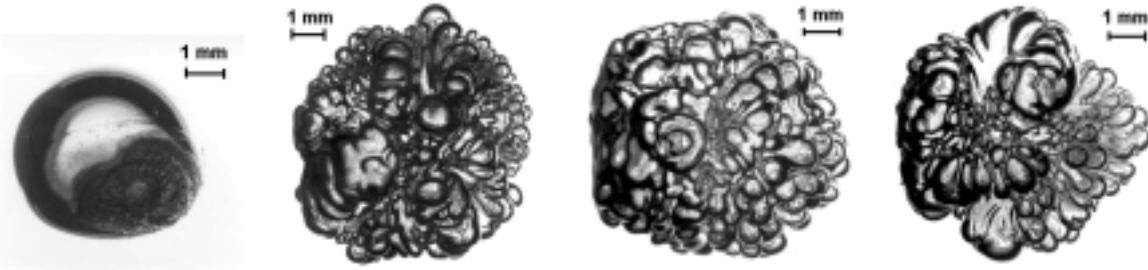


Figure 2: Photographs of ether vapor bubbles in glycerol. From left to right: a bubble before the first collapse and three examples of bubbles after the first collapse (reproduced with permission from Frost (1985)).

Though the evidence is limited, the qualitative agreement between the theoretical value of  $n_m = 41$  and the experimental values around  $n_m = 20$  is encouraging. Clearly, however, further comparisons are necessary to validate the theory.

## 7 Effective Damping

Calculations of the global dynamics,  $R(t)$ , which use the Rayleigh-Plesset equation and therefore assume spherical symmetry require an estimate of the energy dissipation in order to yield realistic results. The dissipation can have a number of physical origins including viscous dissipation in the liquid, thermal effects at the bubble surface and acoustic radiation (Chapman and Plesset 1971, Nigmatulin *et al.* 1981, Prosperetti 1991, Matsumoto and Takemura 1994). However, when any of these techniques are applied to cavitating bubble dynamics such as are the subject of this paper, estimates of the damping or effective viscosity always produce far larger and more numerous rebounds than are observed experimentally. It is often remarked that this is because the bubble almost never remains spherical through the first collapse. Experimental observations such as those of Lauterborn and Bolle (1975) and Tomita and Shima (1990) show that though the bubble may remain relatively intact prior to the first collapse. But what emerges from that collapse is either a highly distorted bubble mass or a cloud of bubble fragments. It seems likely that this fragmentation process dissipates substantial energy and therefore may contribute in a major way to the effective damping of the collapse and rebound cycle. Perhaps this is why the observed number of these cycles rarely exceeds three or four. Consequently, the first step is to recall that the viscous term being used in the usual Rayleigh-Plesset equation 1 (where  $\mu_e$  is now an effective viscosity that incorporates several mechanisms of dissipation) implies a rate of dissipation of energy given by  $16\pi\mu_e R(\dot{R})^2$ . If, using the results of section 2, this is integrated over the collapse interval,  $-t^* < t < t^*$ , an expression for the total energy dissipated during that interval emerges:

$$\frac{64\pi\mu_e}{9} \left\{ \frac{R_{min}K(k-1)}{(k+1)^3} \right\}^{\frac{1}{2}} \quad (17)$$

Turning this around, if we estimated the energy,  $E_D$ , dissipated in a collapse as a result of fission then the appropriate value of  $\mu_e$  which should be used to represent the fission dissipation is

$$\mu_e = \frac{9E_D}{64\pi} \left\{ \frac{(k+1)^3}{R_{min}K(k-1)} \right\}^{\frac{1}{2}} \quad (18)$$

The next step is to consider the fission process and to estimate the absorption of energy that occurs during that process. As a part of that process in the next section  $E_D$  will be connected to the number of fission fragments,  $n_m^3$  or  $n_j^3$ .

## 8 Dissipation mechanisms during fission

There are several mechanisms by which the energy associated with the radial motion may be deflected or dissipated. First, the formation of jets or surface waves will channel kinetic energy in directions in which the

energy must end up being dissipated by viscosity as a result of the fluid mixing and turbulence. Second, the bubble fragments that emerge from the fission process must necessarily contain more surface free energy than the single bubble prior to collapse. This deflection of energy will decrease the kinetic energy associated with the volumetric or radial motion and therefore also contribute to the damping. We shall attempt estimates of both of these contributions to the fission damping.

First we frame the discussion by observing that the kinetic energy,  $E$ , of a single spherical bubble in an infinite fluid is  $2\pi\rho\dot{R}^2R^3$ . Thus, the kinetic energy,  $E^*$ , at the start of the rebound is

$$E^* = 2\pi\rho R_*^3 \dot{R}_*^2 = 2\pi\rho \frac{(k-1)}{k} K \quad (19)$$

To estimate the kinetic energy which might be dissipated due to mixing, we suppose that a single microjet penetrates the single bubble just after the beginning of the rebound when  $R = R^*$  and achieves a velocity that is some multiple,  $C_J$ , of  $\dot{R}_*$  (the work of Blake and Gibson 1987 and others suggests that  $C_J$  may be as high as 10 - see Brennen 1995). Then, if we assume that all the kinetic energy,  $E_J$ , in the jet is dissipated during collapse and that the jet radius is  $1/C_J$  of the bubble radius at the beginning of rebound, it would follow that

$$E_J \propto \pi\rho R_*^3 \dot{R}_*^2 \quad (20)$$

This simply states that the loss is fraction of the total kinetic energy at the start of the rebound. Consequently the radial kinetic energy that remains is also a fraction, say  $\nu$ , of that total kinetic energy. This, in turn, implies that the maximum volumetric radius achieved after the rebound will be  $\nu^{1/3}$  of that achieved before the collapse. If  $\nu$  is some moderate fraction, this implies that only a very small number of collapse and rebound cycles will be observed. Experimental observations such as those of Ellis (1952), Lauterborn and Bolle (1975), Vogel, Lauterborn and Timm (1989) and Tomita and Shima (1990) clearly show that the number of rebounds usually lies between one and three. The plots of Shima and Tomita (1981), for example, suggest that  $\nu^{1/3}$  lies between 0.5 and 0.3 which yields values of  $\nu$  between 0.03 and 0.1. Clearly, in order to quantify this process more accurately requires considerably more information than can be developed here. However, it is encouraging to recognize that the analysis is qualitatively consistent with the experimental observations.

In Brennen (2001), the other drain for kinetic energy, namely the additional surface free energy,  $E_S$ , in the fission fragment cloud is briefly examined and found to be significantly smaller than the estimate of the drain due to fission mixing and turbulence for typical values associated with cavitation in water. However, both energy sinks are orders of magnitude larger than the dissipation due to the conventional spherical bubble mechanisms due to viscous, thermal and acoustic damping. For example, the surface free energy estimate leads to typical effective viscosity values in the range  $0.025 - 0.08 \text{ kg/ms}$  compared with the typical dynamic viscosity of water of  $0.001 \text{ kg/ms}$ .

In summary, we find that both the absorption of energy into surface free energy as a result of fission and the dissipation of energy due to the mixing produced by the non-spherically symmetric motions are much larger than the traditional liquid viscosity contribution to the damping. Moreover, for typical applications to cavitation resulting from micron-sized nuclei in water, the mixing contribution dominates the surface free energy contribution. Only a qualitative examination of this dominant contribution seems possible and that suggests a specific ratio of the maximum bubble size after collapse to that before. At present, it therefore seems practical to examine the experimental observations for an appropriate value of this ratio and to use this in the Rayleigh-Plesset module in larger codes.

## 9 Conclusions

Spurred by the need for multiphase flow models of cavitating flows which incorporate accurate Rayleigh-Plesset models for the bubble dynamics, this paper has examined the deficiencies in the Rayleigh-Plesset calculations which occur during cavitating bubble collapse. Numerous experimental observations have revealed that though a single coherent bubble may enter the very rapid collapse phase, almost invariably what emerges is either a highly distorted bubble or a cloud of smaller bubbles. This paper seeks to elucidate this fission process and begins by qualitatively evaluating the number of fission fragments that would result from (a) a fission process resulting from a Rayleigh-Taylor instability of the interface and (b) a fission process

resulting from a re-entrant jet collapse mechanism. Both mechanisms lead to qualitatively similar fission fragment numbers which depend on several global parameters which are identified.

In seeking some experimental verification of these fission fragment numbers we turn, not to pictures of cavitation bubbles (which almost never have the resolution that would allow the counting of bubbles), but to the beautiful photographs by Shepherd, Frost and Sturtevant of the fission of collapsing ether vapor bubbles in glycerol. The theory and observation of the number of fission fragments are qualitatively similar. However, the observed number of fragments is significantly smaller perhaps because viscous effects on the instability were not incorporated in the theory.

We end the paper by evaluating how the fission process will contribute to the damping of the global volumetric motions that the Rayleigh-Plesset equation is often used to simulate. It is shown that the kinetic energy which is dissipated by the mixing and turbulence associated with fission is much greater than the energy which is deflected into the additional free surface energy. But both are much greater than the energy dissipated by the classical viscous, thermal and acoustic mechanisms normally used to evaluate the bubble damping. Thus the paper concludes that for a Rayleigh-Plesset method to adequately model the global volumetric motions of the bubble or bubble cloud, it is necessary to introduce an energy dissipation mechanism associated with the fission process. The present analysis shows that the best way to do this is to set the kinetic energy emerging from the collapse to some fraction of that entering collapse. However, comparisons with experimental observations are necessary to establish the best value for that fraction.

## Acknowledgements

This paper is dedicated to the memory of my colleague Brad Sturtevant whose enthusiasm and dedication inspired all who knew him. I would also like to thank Joe Shepherd, Tim Colonius and Steve Hoestler for their contributions to this paper.

## References

- Blake, J.R. and Gibson, D.C. (1987). *Ann. Rev. Fluid Mech.*, **19**, 99-124.
- Brennen, C.E. (1995). *Cavitation and bubble dynamics*, Oxford Univ. Press.
- Brennen, C.E. (2001). Fission of collapsing cavitation bubbles. Submitted to *J. Fluid Mech.*
- Chapman, R.B. and Plesset, M.S. (1971). *ASME J. Basic Eng.*, **93**, 373-376.
- Ellis, A. (1952). *Observations on cavitation bubble collapse*. Report No. 21-12, Hydrodynamics Lab., California Institute of Technology.
- Frost, D. (1985). Ph.D. Thesis, California Institute of Technology.
- Frost, D. and Sturtevant, B. (1986). *ASME J. Heat Transfer*, **108**, 418-424.
- Lauterborn, W. and Bolle, H. (1975). *J. Fluid Mech.*, **72**, 391-399.
- Matsumoto, Y. and Takemura, F. (1994). *JSME Int. J.*, **37** (2), 288-296.
- Nigmatulin, R.I., Khabeev, N.S. and Nagiev, F.B. (1981). *Int. J. Heat Mass Transfer*, **24** (6), 1033-1044.
- Plesset, M.S. and Mitchell, T.P. (1956). *Quart. Appl. Math.*, **13**, No. 4, 419-430.
- Prosperetti, A. (1991). *J. Fluid Mech.*, **222**, 587-616.
- Shepherd, J.E. (1980). Ph.D. Thesis, California Institute of Technology.
- Shepherd, J.E. and Sturtevant, B. (1982). *J. Fluid Mechanics*, **121**, 379-402.
- Shima, A. and Tomita, Y. (1981). *Ingenieur-Archiv*, **51**, 243-255.
- Tomita, Y. and Shima, A. (1990). *Acustica*, **71**, No. 3, 161-171.
- Vogel, A., Lauterborn, W. and Timm, R. (1989). *J. Fluid Mech.*, **206**, 299-338.